PALEOCEANOGRAPHY, VOL. 15, NO. 6, PAGES 593-604 DECEMBER 2000

Oxygenation history of bottom waters in the Cariaco Basin, Venezuela, over the past 578,000 years: Results from redox-sensitive metals (Mo, V, Mn, and Fe)

K. M. Yarincik,[1] R. W. Murray,[1] T. W. Lyons,[2] L. C. Peterson,[3] and G. H. Haug[4]

Abstract. We present results from analyses of the redox-sensitive metals Mo, V, Mn, and Fe in sediment recovered from the Cariaco Basin (Ocean Drilling Program Leg 165, site 1002). Results are interpreted in the context of previous studies of $\delta^{15}N$, export production (percent total organic carbon), eolian input, and hemipelagic deposition in the basin. Variations in redox metal ratios over the past ~578,000 years were compared to variations in $\delta^{18}O$ at Milankovitch frequencies and show a strong relationship between glacial-interglacial cycles in sea level, governed by the shallow sills encircling Cariaco Basin, and bottom water oxygen content. During 100 kyr and 41 kyr cyclicity, enrichments of Mo and V occur during highly productive interglacials, indicating bottom water anoxia. During glacials, sediments are less depleted or enriched in Mn and Fe relative to the interglacials, reflecting oxic conditions. During 23 kyr and 19 kyr cyclicity, however, these redox metal patterns are not observed, indicating that the Cariaco Basin responds differently to the higher-frequency climate changes.

1. Introduction

The Cariaco Basin, located on the continental shelf of Venezuela (10°40'N, 65°00'W) (Figure 1), is an east-west trending pull-apart basin [*Schubert*, 1982] which consists of two 1400 m deep basins separated by a 900 m deep saddle. The high sedimentation rate (~30 cm/kyr) [*Peterson et al.*, 1999] results in rapid burial of well-preserved sediments on the basin floor, and therefore the Cariaco Basin has developed into one of the premier marine records targeted for high-resolution paleoceanographic and paleoclimatic study, particularly for low-latitude settings. This record is based on material recovered by Ocean Drilling Program (ODP) Leg 165 as well as by previous workers [*Peterson et al.*, 1991, 1999; *Hughen et al.*, 1996a, 1996b; *Lin et al.*, 1997; *Haug et al.*, 1998; *Dean et al.*, 1999; *Werne et al.*, 2000; *Yarincik et al.*, 2000, and references therein].

The basin is currently anoxic below a water depth of ~300 m, the onset of which occurred at ~12.6 ^{14}C kyr [*Peterson et al.*, 1991; *Hughen et al.*, 1996a, 1996b]. The development of anoxia is facilitated by the shallow banks and shelf topography (<100 m) that surround the basin (Figure 1). The shallow banks affect water circulation and become exposed during maximum sea level lowstands, leaving only two narrow sills sufficiently deep to remain submerged. One of these connections to the open ocean is on the western edge of the basin (146 m); the other is on the northern edge (120 m) between Tortuga and Margarita Island [*Peterson et al.*, 1991, and references therein]. During glacial periods of low sea level and restricted water circulation the influx of seawater from the open Caribbean Sea is primarily from the mixed zone, which is rich in dissolved oxygen but depleted in nutrients and therefore limits primary production. This reduction in productivity results in a decrease in the flux of particulate organic matter to the Cariaco seafloor. Oxic conditions have been hypothesized to exist in the water column at these time periods [*Peterson et al.*, 1991; *Haug et al.*, 1998]. At the onset of interglacial periods the rise of sea level results in an influx of nutrient-rich subthermocline waters that are seasonally upwelled and lead to high levels of primary production in the basin. The high oxygen demand created by primary production cannot be met by the rate of oxygen replenishment in the stratified basin, leading to anoxic conditions [*Peterson et al.*, 1991; *Haug et al.*, 1998; *Peterson et al.*, 1999]. Temporal variability in bulk P concentrations [*Yarincik*, 1999] are consistent with productivity trends inferred from total organic carbon (TOC) concentration [*Haug et al.*, 1998] in that increased P concentrations occur during periods of high percent TOC. Overall, during periods of high surface production and anoxia, the sediments deposited are rich in preserved TOC [*Haug et al.*, 1998; *Peterson et al.*, 1999], are unbioturbated, and contain a higher frequency of distinctly laminated intervals [*Peterson et al.*, 1991; *Hughen et al.*, 1996a, 1996b]. Despite the significance of biogenic influences on the sedimentary record in the Cariaco Basin, however, the sediments nonetheless contain 30-90 weight percent terrigenous matter [*Peterson et al.*, 1999; *Yarincik et al.*, 2000].

Haug et al. [1998] discussed the consequences of sea level change on nutrient supply to the anoxic Cariaco Basin and its impact on production and sedimentary $\delta^{15}N$ and reported that N_2 fixation affects oceanic production on glacial/interglacial timescales. N_2 fixation produces biomass of low $\delta^{15}N$ and is argued to be an important component of the nitrogen cycle in

[1]Department of Earth Sciences, Boston University, Boston, Massachusetts.
[2]Department of Geological Sciences, University of Missouri, Columbia.
[3]Rosenstiel School of Marine and Atmospheric Science, University of Miami, Miami, Florida.
[4]Department of Earth Sciences, Eidgenossische Technische Honschule Zentrum, Zurich, Switzerland.

Paper number 1999PA000401.
0883-8305/00/1999PA000401$12.00

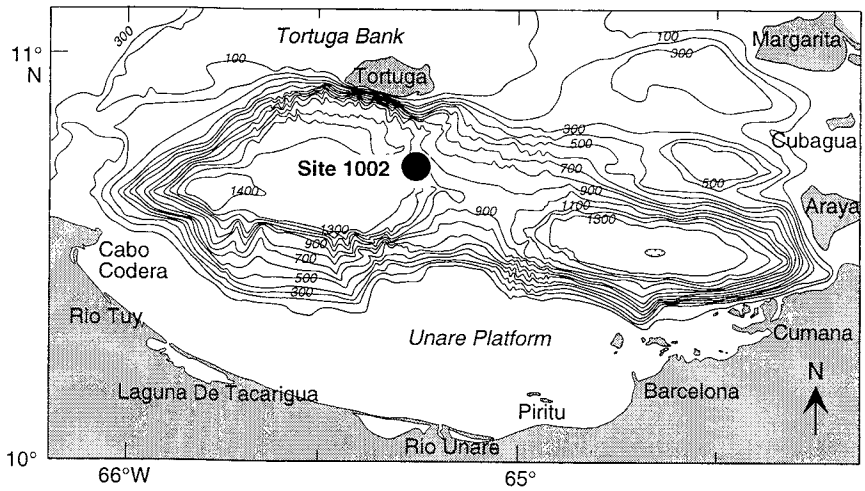

Figure 1. Location of Ocean Drilling Program (ODP) site 1002 (from *Sigurdsson et al.* [1997] and *Yarincik et al.* [2000]). Note relatively shallow sill depths around the basin.

the modern Cariaco Basin [*Walsh*, 1996]. *Haug et al.* [1998] attributed the light interglacial $\delta^{15}N$ values (~2-3‰) observed in the ODP site 1002 record to N_2 fixation. During glacial intervals the sediments are bioturbated (oxic bottom water conditions) with low percent TOC and sedimentary $\delta^{15}N$ values of ~5‰, suggesting that N_2 fixation contributed little to the N nutrition of Cariaco surface waters. The most plausible explanation for the inferred glacial/interglacial changes in N_2 fixation in Cariaco is that they have occurred in response to changes in the relative role of denitrification.

Currently, we cannot discern whether changes in N_2 fixation were driven locally or globally. The spectral phasing of the $\delta^{15}N$ changes appears to support a global driving force. Changes in the $\delta^{15}N$ record lag those of percent TOC and sea level by ~4 kyr [*Haug et al.*, 1998]. Because the oceanic residence time for nitrate is ~3 kyr [*Gruber and Sarmiento*, 1997], a significant NO_3/PO_4 change would take on the order of several thousand years to develop in the global ocean, while it would require much less time (<100 years) [*Deuser*, 1973; *Zhang and Millero*, 1993] to develop locally in the deep Cariaco Basin.

In this paper, we use bulk sedimentary distributions of the redox-sensitive metals Mo, V, Mn, and Fe to show that varying bottom water oxygenation in the Cariaco Basin corresponds to variations in $\delta^{18}O$ and percent TOC (used as a first-order indication of surface water production) and ultimately in response to climatically driven sea level change. We use standard time series analysis [e.g., *Imbrie et al.*, 1992] to quantify the variability in the distributions of redox-metals in the context of climate change. This approach allows for correlation among the various geochemical records while simultaneously documenting the temporal leads and lags in the system to assess the overall chemical-climate response. Glacial periods in the Cariaco Basin are characterized by positive $\delta^{18}O$ (reflecting increased ice volume and low sea level), high $\delta^{15}N$, low percent TOC, and redox metal distributions suggesting oxygenated conditions. Conversely, interglacials are characterized by negative $\delta^{18}O$, low $\delta^{15}N$, high %TOC, and redox metal distributions suggesting anoxic conditions [e.g., *Haug et al.*, 1998, *Peterson et al.*, 1999], although there are differences in redox behavior among the different Milankovitch frequencies of climate variability. We also present high-resolution redox metal data for the most recent glacial-interglacial redox transition (~ 12.6 ^{14}C kyr) in order to better understand the mechanisms of metal partitioning. This work complements our previous study of climatically driven variations in Saharan-derived eolian matter and hemipelagic deposition into the Cariaco Basin [*Yarincik et al.*, 2000].

2. Redox-Sensitive Metals

Concentrations of redox metals in marine sediment are influenced by variations in the oxygenation of the water column, the oxygenation of the bottom water (along with the uppermost 1-2 cm of sediment), the concentration of the given metals in the biogenic sources, and the portion of the detrital inventory that is refractory. In order to isolate the effects of bottom water oxygenation, it is necessary to consider distributions of multiple redox-sensitive elements, which ideally include metals that respond differently to the redox state of the given system. As summarized by *Morford and Emerson* [1999] (Figure 2), the distributions of the major elements Mn and Fe, along with those of the redox-sensitive trace metals Mo, V, U, Re, and Cd, can yield powerful information linked to local or global environmental variability.

We have studied variations in bottom water oxygenation of Cariaco Basin that are recorded in distributions of the redox-sensitive elements Mn, Fe, Mo, and V. Both Mn and Fe are more soluble in their reduced states [*Scoullos*, 1983; *Jacobs et al.*, 1987; *Landing and Bruland*, 1987; *Burton and Statham*, 1988; *Calvert and Pedersen*, 1993; *Piper*, 1994; *Crusius et al.*, 1996; *Morford and Emerson*, 1999, and references therein], and thus their particulate concentrations in the bulk sediment should in theory be lower during periods of water column anoxia. In practice, these relationships are complicated by the formation of diagenetic and syngenetic phases such as pyrite,

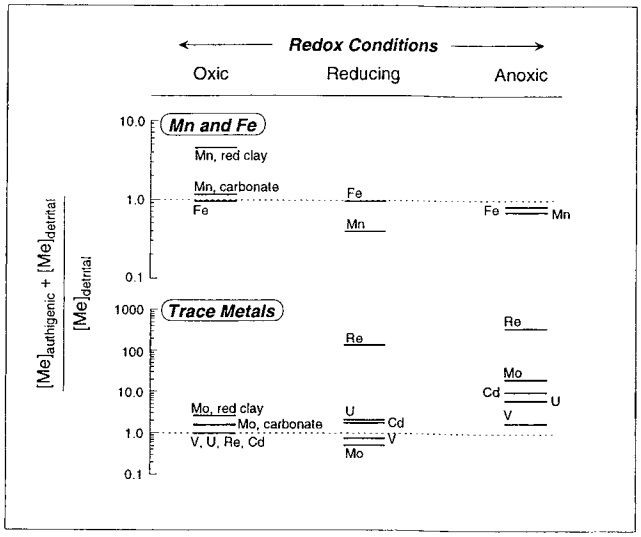

Figure 2. Enrichment and depletion factors for redox-sensitive metals in marine sediment (from *Morford and Emerson* [1999] and based on references therein).

as discussed below. Mn is more labile than Fe and during reducing and anoxic conditions can be dissolved from the bottom sediment and diffused into the overlying anoxic water column, leading to concentrations that are depleted with respect to average shale (Figure 2). Although Fe responds in a similar fashion to anoxia, owing to its greater detrital inventory as well as its strong tendency to be retained as iron sulfide the depletion is not as sensitively documented as in the case of Mn (Figure 2). Conversely, concentrations typical of average shale or enrichments of Mn and Fe (depending on the host lithology) are indicative of relative bottom water oxygenation. The decoupling between the Fe and Mn behaviors will be capitilized upon here to elucidate the relative timings of the onset of the different degrees of oxygen depletion and changes in sediment provenance that control the distributions of these two metals in sediments of the Cariaco Basin.

The opposite trend is seen for Mo and V, the solubility of which decrease in the reduced state [*Jacobs et al.*, 1987; *Francois*, 1988; *Emerson and Huested*, 1991; *Calvert and Pedersen*, 1993; *Jones and Manning*, 1994; *Piper*, 1994; *Piper and Isaacs*, 1995; *Dean et al.*, 1997, 1999; *Morford and Emerson*, 1999, and references therein]. Overall, these elements should be enriched in the sediment during periods of anoxia and depleted from sediment during periods of bottom water oxygenation. Although Mo and V both behave conservatively in seawater [*Burton and Statham*, 1988; *Emerson and Huested*, 1991; *Calvert and Pedersen*, 1993], Mo is particularly useful for studies of bottom water oxygenation because its seawater concentration is higher than that of other heavy metals [*Piper*, 1994]. Accordingly, Mo is the more sensitive of the two elements, recording stronger enrichments above average shale values during anoxic conditions than does V [e.g., *Morford and Emerson*, 1999] (Figure 2). An excellent example of the utility of Mo distributions has been provided by *Dean et al.* [1999], who demonstrated that Mo accumulation in the Cariaco Basin over the past 24 kyr increased during periods of elevated primary production.

Because the nature of the age model for the long ODP record at site 1002 precludes the calculation of elemental accumulation rates (as described below), our approach is to study the distributions of Mo, V, Mn, and Fe with respect to their terrigenous inventory by normalizing the concentrations of the redox-sensitive metals to the concentration of Al in the same sample [e.g., *Calvert and Pedersen*, 1993; *Dean et al.*, 1997]. We compare temporal variability in these Al-normalized ratios to their values in average shale (e.g., Post-Archean Average Shale (PAAS)) [*Taylor and McLennan*, 1985] in order to identify elemental enrichment or depletion. This assumes that the entire Al inventory is contained in the detrital component (as opposed to adsorbed) [*Murray and Leinen*, 1996; *Dymond et al.*, 1997], which is appropriate considering the dominantly terrigenous nature of Cariaco Basin sediments [*Peterson et al.*, 1999; *Yarincik et al.*, 2000]. We specifically do not use Ti as the normalizing element owing to the presence of an eolian source of rutile (TiO_2) in Cariaco sediment, input of which has been shown to vary strongly in concert with glacial-interglacial climate state [*Yarincik et al.*, 2000]. To summarize, our overall strategy is to infer bottom water oxygenation conditions on the basis of the redox metal ratios, capitilizing on the contrasting behavior within and between the Fe-Mn and Mo-V redox pairings. In the most general sense, elevated values of Mo/Al and V/Al reflect bottom water anoxia, while increased Mn/Al and Fe/Al are indicative of oxic bottom water conditions. Gradations between these elemental ratios can potentially be used to temporally identify the gradations in the onset of the differing redox states of the bottom waters.

3. Trace Metal Trends Across the Most Recent Oxic-Anoxic Transition

Characterization of the most recent redox transition in the Cariaco Basin enhances the utility of tracemetal approaches to addressing longer-term paleoceanographic variability. An ongoing high-resolution evaluation of the redox transition at 12.6 ^{14}C kyr (~15 calendar kyr) [*Lyons et al.*, 1998, manuscript in preparation, 2000], at which occurs the most recent glacial-interglacial transition [*Peterson et al.*, 1991; *Hughen et al.*, 1996a, 1996b; *Lin et al.*, 1997], provides critical calibration of the method that we apply to the 578 kyr record. Results for bulk Mn, Fe, Mo, and V are compared to variations in percent TOC (Figure 3). These data reveal comparatively small variation in Mn/Al and Fe/Al ratios across the abrupt redox interface that marks the progression from oxic to anoxic-sulfidic deposition. This transition reflects increased nutrient fluxes linked to rising sea level and corresponding increases in productivity and water column oxygen demand (as cited above). Two additional relationships are indicated: (1) the Mn/Al and Fe/Al ratios within the oxic sediments are either equal to or slightly greater than those of the laminated sediments, and (2) there appears to be diagenetic remobilization of these metals associated with the onset of water column anoxia, including effects linked to the downward diffusion of dissolved sulfide.

Manganese and Fe are commonly lost from sediments via diffusion into an overlying anoxic water column or through dissolution of particulate oxyhydroxides settling within the reducing water column, both of which drive Mn/Al and Fe/Al

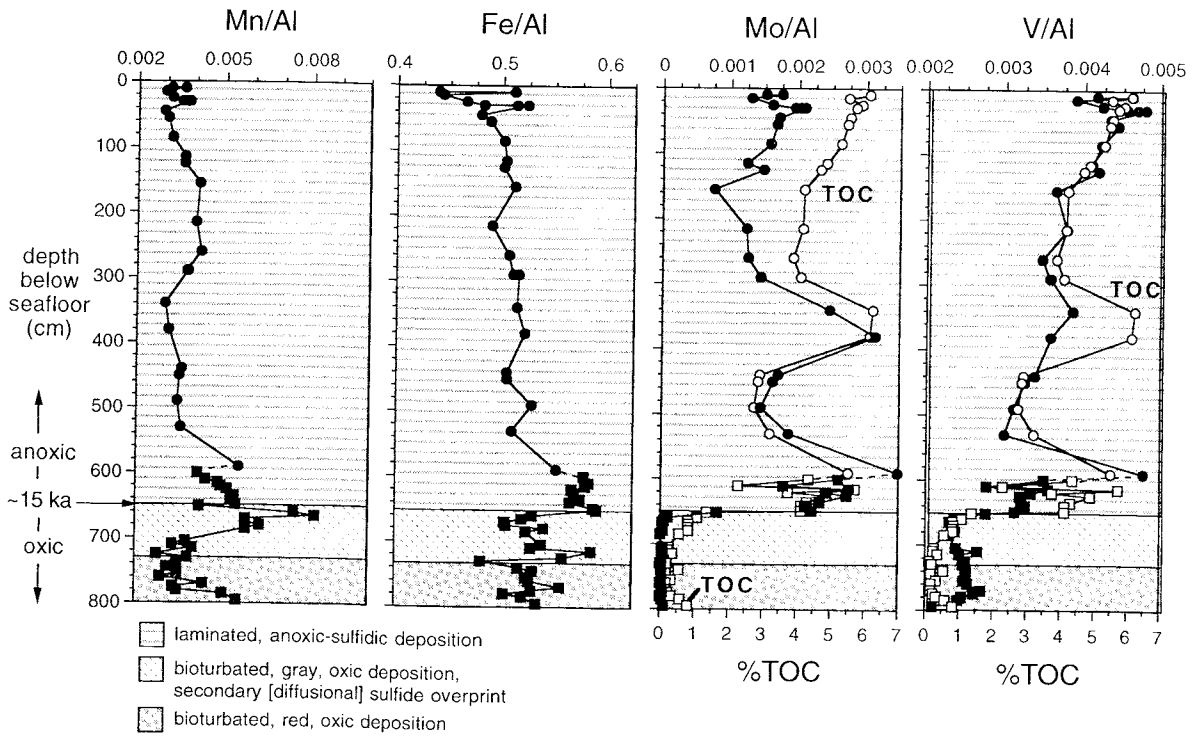

Figure 3. Down core trends for Mn/Al, Fe/Al, Mo/Al and V/Al in the upper 8 m of sediment at site 1002. The open and solid circles represent percent total organic carbon (TOC) and metal/Al ratios, respectively, from hole 1002B. The open and solid squares reflect percent TOC and metal/Al ratios, respectively, from hole 1002A. The two data sets were spliced together using magnetic susceptibility records. The plots include the transition from oxic to anoxic-sulfidic deposition at 12.6 ^{14}C kyr (15 calendar kyr). The uppermost oxic sediments were diffusionally overprinted by sulfide following the onset of anoxic-sulfidic conditions in the water column. After *Lyons et al.* [1998, unpublished data, 2000].

ratios lower [*Calvert and Pedersen*, 1993]. Nevertheless, predicted Mn and Fe depletions can be complicated by an abundance of refractory, detritally delivered Fe and Mn phases that are not easily remobilized [*Canfield*, 1989; *Canfield et al.*, 1992] or through the formation of secondary phases that facilitate the retention of the metals (e.g., pyrite and Mn-carbonates). In fact, studies in other anoxic settings, such as the Black Sea, suggest that ratios of reactive-to-total Fe and Fe/Al can actually be driven upward by the scavenging of dissolved Fe in the anoxic-sulfidic water column during the syngenetic formation of pyrite [*Canfield et al.*, 1996; *Lyons*, 1997; *Raiswell and Canfield*, 1998]. Under conditions of slow terrigenous sedimentation, this Fe augmentation via scavenging can enrich the sediments in Fe relative to the terrigenous component since the scavenged reactive Fe is decoupled from the local terrigenous flux. This effect is not evident in the laminated sediments depicted in Figure 3 because of the comparatively rapid terrigenous sedimentation in the Cariaco Basin, which swamps any signal of scavenging. Redistribution of Mn and Fe occurs diagenetically in sediments of oxic basins (e.g., the Mn pump described by *Calvert and Pedersen* [1993]), but in such cases the overall Mn and Fe concentrations still reflect the terrigenous input.

Clearly, concentration trends for Fe and Mn are not linked in a simple way to the redox conditions in the overlying water column or to the availability of organic matter (since much of the redox cycling and fixation of these metals can occur in an anoxic water column independent of the local flux of TOC) [*Lyons and Berner*, 1992]. These caveats are particularly relevant at sites of rapid terrigenous deposition with large amounts of refractory Mn and Fe. This observation, based here on the short-term record, will also be seen to hold true in the longer, 578 kyr record discussed later in this paper.

Molybdenum and V, on the other hand, show unambiguous relationships to depositional redox that are likely manifested across the 578 kyr sediment record. First, Mo/Al and V/Al ratios increase abruptly across the redox interface (Figure 3) [*Lyons et al.*, 1998; *Dean et al.*, 1999]. In the sediments deposited under oxic conditions, regardless of the presence or absence of a diagenetic sulfide overprint, the ratios are low and independent of percent TOC. Under anoxic-sulfidic conditions the high ratios for both metals track percent TOC, confirming that the extent of enrichment can vary substantially under persistently anoxic conditions. Ultimately, Mo and V enrichments are favored by high activities of HS^- in an anoxic water column [*Breit and Wanty*, 1991; *Helz et al.*, 1996]. Beyond reactions between the metals and dissolved sulfide, the presence of high HS^- activities also facilitates the scavenging of Mo and V by organic matter in the water column. For example, Mo enrichments are, in simple terms, strong when the water column is sulfidic, at which point the Mo/Al ratio also closely tracks the percent TOC (Figure 3) [*Lyons et al.*, 1998], and the ratio is low and independent of percent TOC under oxic conditions. Analogous relationships are suggested for V/Al (Figure 3), suggesting that Mo and V enrichments are intimately coupled to TOC accumulation in the Cariaco Basin

under strongly reducing conditions but could be less so in the absence of appreciable HS^-, even in the presence of low depositional oxygen and high percent TOC. Such relationships both enhance and complicate the utility of Mo and V as simple proxies for anoxia and likely contribute to some of the variability shown below in the 578 kyr record. For example, percent TOC (and thus Mo/Al and V/Al) can vary substantially during extended episodes of anoxic-sulfidic deposition as a function of temporal trends in productivity (e.g., the Younger Dryas) and terrigenous dilution [*Werne et al.*, 2000].

4. Methods

4.1. Inductively Coupled Plasma Emission Spectrometry

Sediment dissolution procedures are described by *Yarincik* [1999] and *Yarincik et al.* [2000] and follow a procedure similar to that of *Murray and Leinen* [1996] (although modified owing to the refractory nature of the relatively terrigenous-rich sediments of Cariaco). Once the samples were completely digested by a combined sealed beaker $HF\text{-}HNO_3\text{-}HClO_4\text{-}HCl$ acid attack, solutions were diluted thousandfold and hundredfold for major and trace element analyses, respectively, and analyzed using a Jobin Yvon JY 170C Ultrace inductively coupled plasma emission spectrometer (ICP-ES) to determine concentrations of Al (λ = 308.215 nm, and blank determined detection limit (BDDL) equals 0.03 weight percent), Mn (λ = 257.610 nm, and BDDL equals 2 ppm), Fe (λ = 238.204 nm, and BDDL equals 0.009 weight percent), Mo (λ = 202.030 nm, and BDDL equals 3 ppm), and V (λ = 292.402 nm, and BDDL equals 2 ppm). Data were acquired in sequential mode using background corrections as appropriate.

Two hundred forty samples were analyzed in random depth order in nine batches over a period of several months. As described by *Yarincik* [1999] and *Yarincik et al.* [2000], a homogenized natural sample of typical Cariaco Basin sediment was analyzed with each batch as an internal reference and to determine analytical precision. Using this approach, precision of 2% of the measured value was obtained for Mn/Al (0.0033 ± 0.0001) and Fe/Al (0.51 ± 0.01), precision of 3% was obtained for V/Al (0.0029 ± 0.0001), and precision of 8% was obtained for Mo/Al (0.0014 ± 0.0001). A standard reference sediment (BCSS-1, an estuarine sediment from Baie des Chaleurs in the Gulf of St. Lawrence) was also analyzed with each batch to confirm analytical accuracy. Accuracy of the measurements was within precision, although this could not be checked for Mo since concentrations in BCSS-1 are below the detection limit. Chemical data are provided in Table A1 and shown in Figure 4.[1]

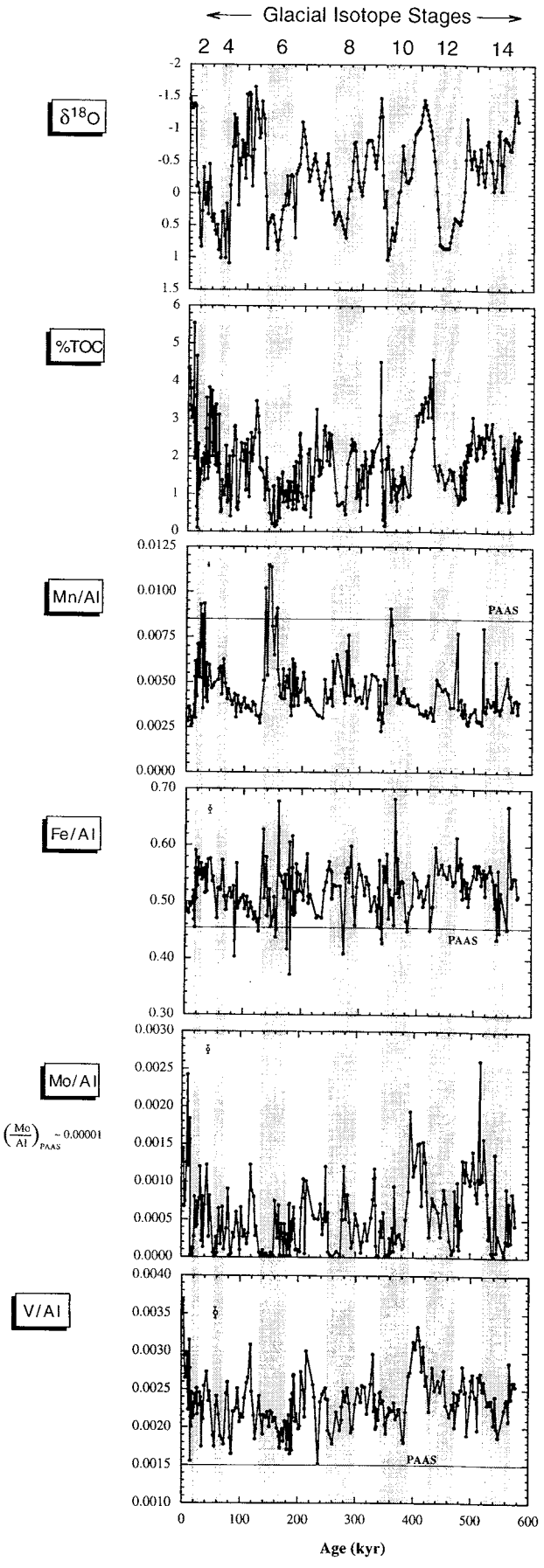

Figure 4. Down hole variations in $\delta^{18}O$, percent TOC, and Al-normalized redox metal ratios versus age for the Cariaco Basin sedimentary record at site 1002. Values of Al-normalized ratios in Post-Archean Average Shale (PAAS) are given in each panel. Representative analytical uncertainties are given in the top left-hand corner of each panel. Glacial marine isotope stages (shaded) are from *Imbrie et al.* [1984].

Table 1. Results of Cross-Spectral Analysis, ODP Site 1002, Cariaco Basin [a]

	Phase Difference ± Phase Error ; Coherency ; Kyr Lead or Lag			
Variable 1 vs. Variable 2	100 kyr	41 kyr	23 kyr	19 kyr
$\delta^{18}O$ vs. SPECMAP	2 ± 9 ; 0.94	-8 ± 8 ; 0.95	5 ± 9 ; 0.95	2 ± 8; 0.95
%TOC vs. $\delta^{18}O$	-146 ± 11; 0.92 ; 41	177 ± 11; 0.91 ; 20	132 ± 22 ; 0.74 ; 8	
Mn/Al vs. $\delta^{18}O$	-4 ± 14; 0.88 ; 1	55 ± 19; 0.80 ; 6		
Fe/Al vs. $\delta^{18}O$	23 ± 23; 0.72 ; 6		49 ± 25; 0.70 ; 3	25 ± 24; 0.71 ; 1
Mo/Al vs. $\delta^{18}O$	-152 ± 18; 0.81 ; 42	190 ± 14; 0.87 ; 22	140 ± 17; 0.82 ; 9	
V/Al vs. $\delta^{18}O$	221 ± 6; 0.97 ; 61	161 ± 26; 0.68 ; 18		
Mn/Al vs. %TOC	140 ± 19; 0.79 ; 39	-136 ± 26; 0.68 ; 15		
Fe/Al vs. %TOC			-55 ± 21; 0.76 ; 3	-37 ± 20; 0.78 ; 2
Mo/Al vs. %TOC	-6 ± 7; 0.96 ; 2	11 ± 16; 0.85 ; 1	-3 ± 13; 0.89 ; 0	
V/Al vs. %TOC	6 ± 8; 0.93 ; 2	12 ± 23; 0.73 ; 1		-18 ± 25; 0.70 ; 1
V/Al vs. Mo/Al	11 ± 15; 0.86 ; 3	10 ± 15; 0.85 ; 1		-98 ± 18; 0.81 ; 5
Fe/Al vs. Mn/Al	16 ± 22; 0.74 ; 4		-78 ± 25; 0.69 ; 5	
Mo/Al vs. Mn/Al	-146 ± 26; 0.68 ; 40			
V/Al vs. Mn/Al	-135 ± 17; 0.83 ; 38			

[a] Positive phase angles indicate that the first variable leads the second. Coherency equals 0.64 at the 80% confidence level. No phase angle is given if records are not coherent at the 80% confidence level or if one variable shows no increase in variance centered at the period of interest. "Kyr Lead or Lag" is calculated by [(Phase Difference)/360 x frequency]. Interpolation and cross-spectral analyses performed for 287 samples at Δt = 2 kyr for 572 kyr. Bandwidth is 0.007 with 95 lags. Here vs. is versus and %TOC is percent total organic carbon.

4.2. Age Model, Supporting Data, and Time Series Analysis

The oxygen isotope ($\delta^{18}O$) data and age model for the 0 to ~580 kyr record of ODP Site 1002 are from *Peterson et al.* [1999]. Cross-spectral analysis (detailed below) of Site 1002 $\delta^{18}O$ versus the SPECMAP $\delta^{18}O$ standard show high coherence and phase locking at all Milankovitch frequencies (Table 1). The average age resolution between samples in this study is ~2.4 ± 2 kyr. Interpolation and treatment of disturbed core sections are described by *Yarincik et al.* [2000] and followed procedures of *Peterson et al.* [1999]. The age model is based on a record of *Globigerinoides ruber* which is insufficiently resolved to calculate elemental mass accumulation rates with confidence [*Haug et al.*, 1998]. Consequently, accumulation rates of the trace metals are not discussed. The percent TOC data are from *Haug et al.* [1998].

Variations in the Al-normalized elemental ratios are compared to variations in $\delta^{18}O$, a proxy for global ice volume and sea level change, via cross-spectral analyses [e.g., *Imbrie et al.*, 1992] performed using the ARAND software package from Brown University. In such analysis, a metal ratio that covaries "in phase" with positive $\delta^{18}O$ reaches maximum values during glacial periods, as $\delta^{18}O$ is higher during glacials. Conversely, if a ratio is in phase with negative $\delta^{18}O$ (which is also 180° out of phase with positive $\delta^{18}O$), the ratio is highest during interglacials. Details of the statistical treatments are provided in Table 1, as are data for the relative phasings of the records as temporal "leads" or "lags." Phase angles in Table 1 are expressed relative to positive $\delta^{18}O$. However, at various points in the discussion below where the phase angles are close to positive or negative 180°, we discuss the phase relationships with respect to negative $\delta^{18}O$. Coherence plots of the cross-spectral relationships are provided in Figure 5, which compares the spectral behavior of $\delta^{18}O$ to that of the Al-normalized redox metal ratios, and in Figure 6, which compares the spectral behavior of percent TOC to the redox metal ratios. The statistical relationships are further presented in a "phase wheel" (Figure 7), which plots the phase angle data from Table 1 in a form that allows for visualization of the similarities and differences in the cross-spectral character of the different variables.

5. Results

5.1. $\delta^{18}O$ and TOC

The temporal patterns of percent TOC at Hole 1002C provide a first-order assessment of the relationship between redox conditions and productivity and help provide a framework for the interpretations of redox metals. Cross-spectral analysis shows that percent TOC is strongly coherent with negative $\delta^{18}O$ at the 100 and 41 kyr frequencies, with coherencies of ~0.91 in both cases, and only moderately coherent at 23 kyr (Table 1). The phase relationships indicate that in the 100 kyr band percent TOC lags behind negative $\delta^{18}O$ (that is, interglacials) by ~ 35° of phase angle (corresponding to a 9 kyr lag). The percent TOC is exactly in phase with negative $\delta^{18}O$ in the 41 kyr band and leads negative $\delta^{18}O$ by ~ 8 kyr in the 23 kyr band (Table 1 and Figure 7). This agrees with the finding of *Haug et al.* [1998] that percent TOC generally increases during interglacial periods and is

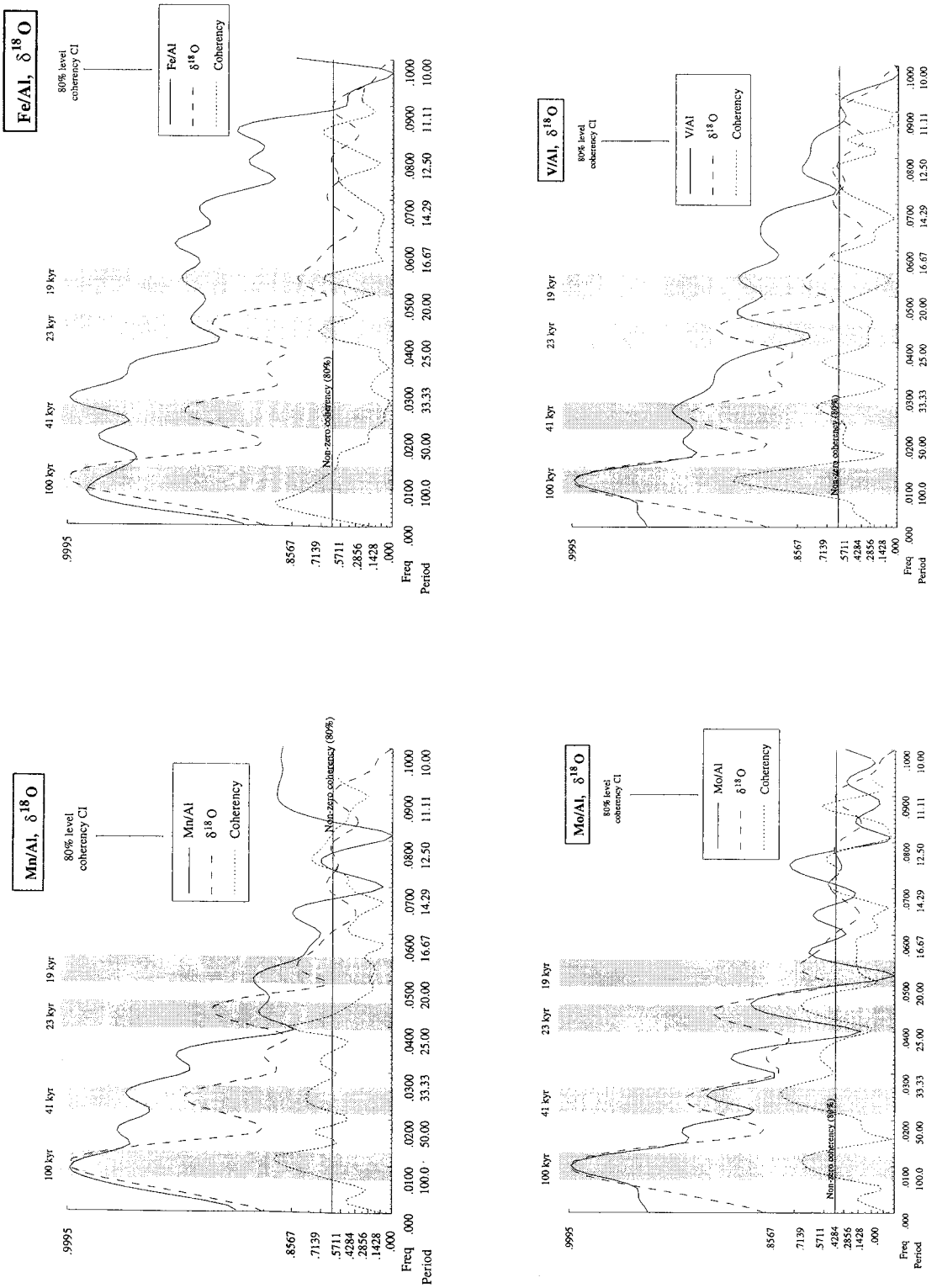

Figure 5. Coherence plots resulting from cross-spectral analyses of each Al-normalized redox metal ratio versus $\delta^{18}O$, site 1002. See also Table 1 and Figures 6 and 7.

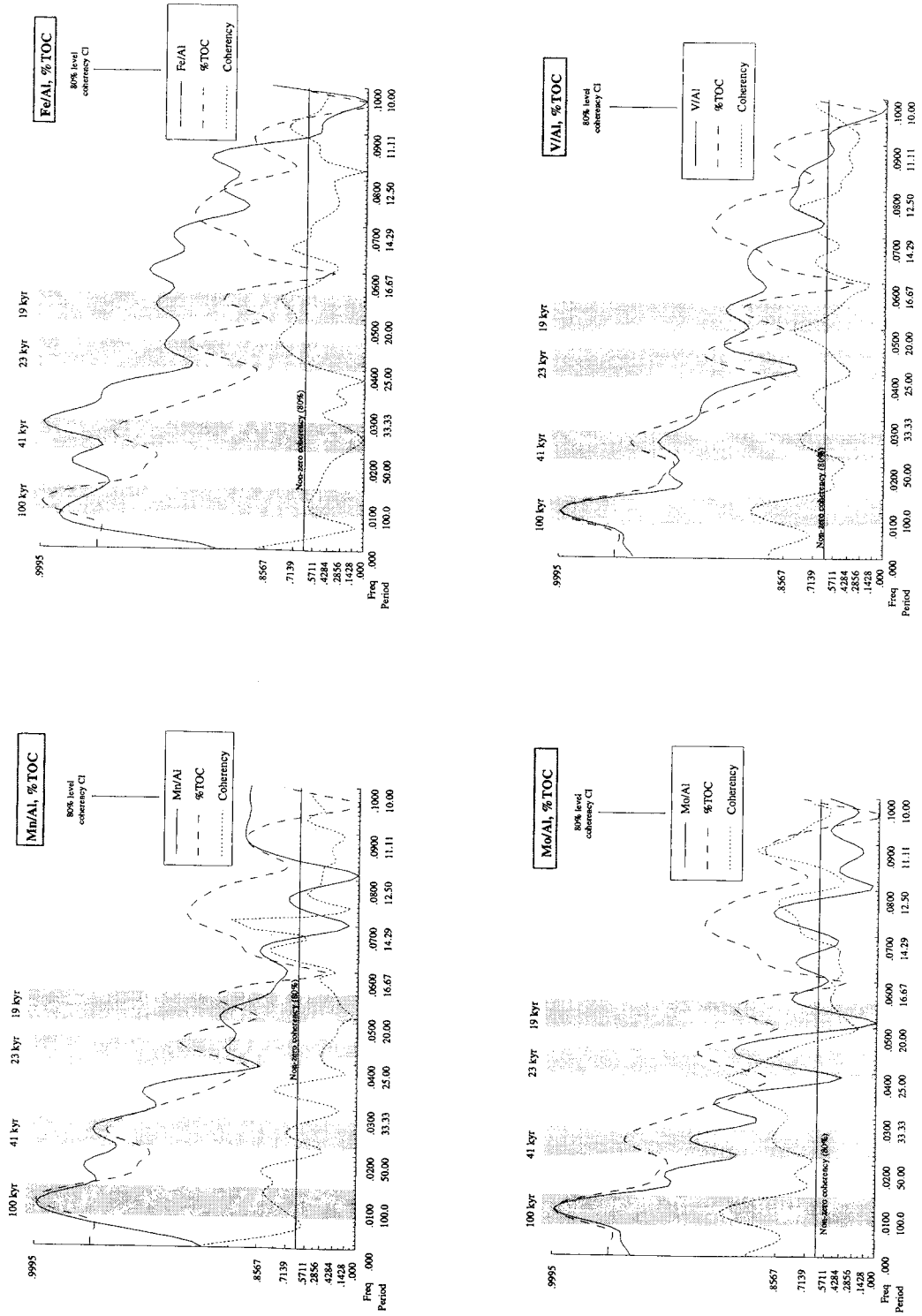

Figure 6. Coherence plots resulting from cross-spectral analyses of each Al-normalized redox metal ratio versus percent TOC, site 1002. See also Table 1 and Figures 5 and 7.

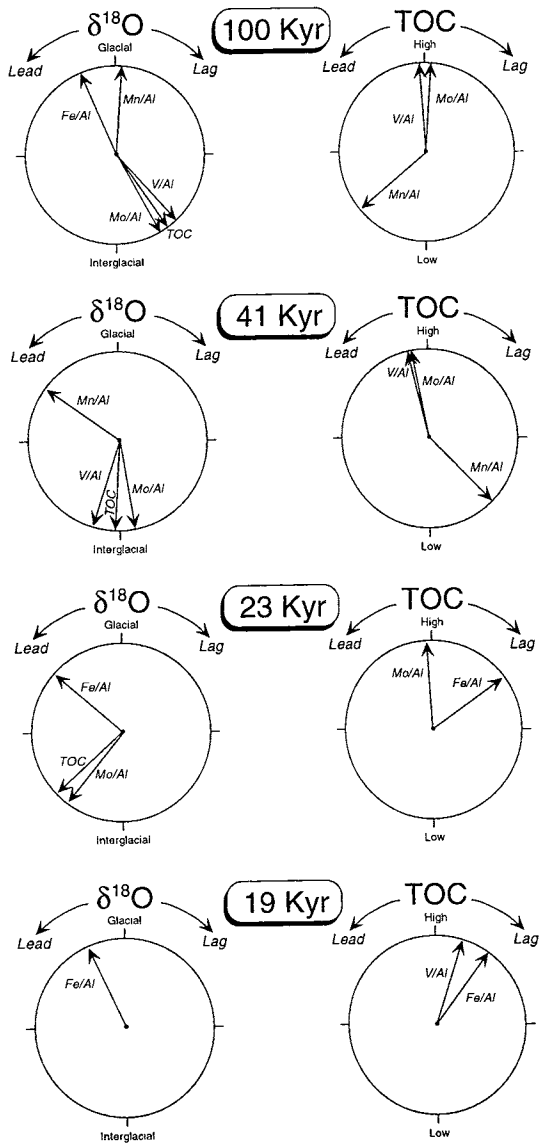

Figure 7. Phase wheel diagrams for $\delta^{18}O$ and percent TOC. For $\delta^{18}O$, in-phase relationships with glacial climate states are represented at top of each wheel, while in-phase relationships with interglacial climate states are represented at the bottom of each wheel. Analogously, high TOC conditions are represented at top of each wheel, with low TOC at the bottom. Vectors represent phase angles given in Table 1. Note uncertainty values in Table 1, which are not plotted here. Note general similarity in behavior in the 100 kyr and 41 kyr bandwidths, whereas the 23 kyr and 19 kyr bandwidths display different behavior.

dominantly controlled by sea level changes: high sea level stands allow the influx of nutrient-rich thermocline waters from the Caribbean Sea. The lag and lead at 100 kyr and 23 kyr, respectively, indicate that at these frequencies the accumulation of TOC is not related solely to the sea level-mediated delivery of nutrients to the surface water and may be responding to other processes (e.g., enhancement of burial efficiency due to variations in sedimentation rate).

5.2. Redox Sensitive Metals

Values for Mn/Al range from 0.0023 to 0.0115 and average 0.0045 ± 0.002 (Figure 4 and Table A1). For much of the record, values are significantly less than that of PAAS (~0.0085) [*Taylor and McLennan*, 1985]. Values for Fe/Al range from 0.37 to 0.68, averaging 0.52 ± 0.07, and are generally greater than that of PAAS (~0.43) [*Taylor and McLennan*, 1985] for most of the record (Figure 4 and Table A1). Both sedimentary Mn/Al and Fe/Al tend to be comparatively high during glacial periods.

Mo/Al ranges from below detection limit of Mo (see above) to 0.0026 and average 0.00052 ± 0.0005 (Figure 4 and Table A1). Mo/Al values also tend to be greater than values in PAAS (1×10^{-5}) [*Taylor and McLennan*, 1985]. Values for V/Al range from 0.0015 to 0.0037 and average 0.0023 ± 0.0003 (Figure 4 and Table A1), which are generally higher than the value of PAAS (~0.0015) [*Taylor and McLennan*, 1985].

In the 100 kyr frequency, spectral analyses show coherence of all redox metal/Al ratios with respect to variation in $\delta^{18}O$ (Figure 7 and Table 1). Mn/Al and Fe/Al ratios are both in-phase with positive $\delta^{18}O$ at this frequency. Mo/Al slightly leads $\delta^{18}O$ (by ~8 kyr), while V/Al lags behind negative $\delta^{18}O$ by ~40° of phase angle (~11 kyr). Mn/Al, Mo/Al, and V/Al values also show strong coherence with percent TOC at the 100 kyr frequency (Figure 7 and Table 1). Mn/Al leads percent TOC by ~140° of phase angle (~39 kyr), while both Mo/Al and V/Al are exactly in phase and highly coherent with percent TOC (Figure 7).

In the 41 kyr frequency, Fe/Al ratios show no significant relationship with $\delta^{18}O$, while all other redox metal ratios are more strongly coherent, although not generally as strong as they are at 100 kyr (Table 1). Mn/Al leads positive $\delta^{18}O$ by 55° of phase angle (~6 kyr), although the coherency is not strong. Both Mo/Al and V/Al are exactly out of phase with positive $\delta^{18}O$, with Mo/Al being strongly coherent with $\delta^{18}O$ (0.87) and V/Al being barely coherent at the 80% confidence level. Mn/Al is weakly coherent with percent TOC in the 41 kyr band and lags behind it by ~140° of phase angle (~15 kyr). Mo/Al and V/Al remain coherent and in phase with percent TOC in this frequency, again with Mo/Al being strongly coherent (0.85).

In the 23 kyr frequency, Mn/Al and V/Al show no relationship to either $\delta^{18}O$ or percent TOC. Fe/Al only slightly leads positive $\delta^{18}O$ and lags percent TOC with weak coherency in both cases. Mo/Al and $\delta^{18}O$ are more strongly coherent at this frequency (0.82), with Mo/Al leading positive $\delta^{18}O$ by ~140° of phase angle (~9 kyr). Mo/Al is also strongly coherent (0.89) and in phase with percent TOC (Figure 7).

In the 19 kyr frequency, there are very few statistically significant relationships (Table 1 and Figure 7). Fe/Al is weakly coherent (with high uncertainty) and in phase with positive $\delta^{18}O$. Fe/Al and V/Al are weakly coherent with percent TOC, with Fe/Al slightly lagging percent TOC and V/Al approximately in phase with percent TOC.

Cross-spectral analyses were also performed to compare the redox metal/Al ratios to each other. All ratios are coherent in the 100 kyr band, with Fe/Al and Mn/Al being in phase and V/Al and Mo/Al also being in phase. There are slight leads and lags between the various combinations of these two pairs of ratios. Visually, the Mo/Al and V/Al curves follow each other closely (Figure 4), and the cross-spectral analysis confirms this in the 100 kyr and 41 kyr bands (Table 1). In the 19 kyr frequency, V/Al lags Mo/Al by ~100° of phase angle (~5 kyr),

while there is no coherence between V/Al and Mo/Al in the 23 kyr frequency. Fe/Al and Mn/Al are weakly coherent (0.69) at 23 kyr but are unrelated at 43 kyr and 19 kyr. In summary, considering all frequencies, the Mo/Al and V/Al curves appear to covary, as do the curves of Fe/Al and Mn/Al. Mo/Al and V/Al inversely follow Mn/Al (Figure 4). In the context of the high uncertainties, these spectral comparisons confirm the visual inverse relationships between Mo/Al and Mn/Al and between V/Al and Mn/Al.

6. Discussion

Our data for redox-sensitive metals at ODP site 1002 show periodic variations in water column oxygenation in Cariaco Basin that correspond to glacial-interglacial climate state, as constrained independently by percent TOC and $\delta^{18}O$. Interglacial periods are characterized by water column anoxia, as indicated by maxima in sedimentary Mo/Al and V/Al, while oxic conditions, indicated by maxima in sedimentary Mn/Al and Fe/Al, correspond to glacial periods. All of the redox metals as well as percent TOC show the most consistent and strongest (in terms of coherence) behavior in the 100 kyr frequency band. In the Cariaco Basin the influx of eolian material as well as variation in the hemipelagic deposition of locally-derived clays are also dominated by variation in the 100 kyr band [*Yarincik et al.*, 2000]. This consistency of variation of redox behavior, eolian input, and local erosion speaks to the dominance of the eccentricity cycle on the paleoclimatic evolution of the Cariaco Basin.

Maxima in Mo concentrations in sediments have commonly been interpreted to reflect anoxic sedimentary depositional environments. Because of the conservative behavior of Mo [*Burton and Statham*, 1988; *Emerson and Huested*, 1991; *Calvert and Pedersen*, 1993] and its relatively high concentration (10 ppb) compared to other trace metals in seawater [*Piper*, 1994, and references therein], Mo is the least ambiguous and most useful element for interpreting paleoredox conditions [*Jacobs et al.*, 1987; *Emerson and Huested*, 1991; *Piper*, 1994; *Piper and Isaacs*, 1995; *Crusius et al.*, 1996; *Dean et al.*, 1997, 1999]. Mo is considerably more enriched with respect to average shale than any other element, including V, in sediments of anoxic basins [*Jacobs et al.*, 1987; *Morford and Emerson*, 1999, and references therein]. Consistent with this, Mo/Al in the Cariaco Basin is strongly coherent with and has minimum phase angle between $\delta^{18}O$ and percent TOC at the 100 kyr and 41 kyr Milankovitch frequencies. Moreover, Mo/Al trends document increased sedimentary accumulation of Mo during highly productive interglacial periods. These relationships provide independent corroboration of the results of *Peterson et al.* [1991, 1999] and *Haug et al.* [1998] and indicate climatically driven variations in anoxia. The strong coherency and inverse relationship of Mo/Al with $\delta^{18}O$ at the 100 kyr and 41 kyr periodicities indicates changes in basin oxygenation linked to sea level. Similarly, the strong coherence and relationship of Mo/Al with percent TOC confirms that the accumulation of TOC is occuring during oxygen-depleted conditions.

The V/Al data confirm the overall interpretations suggested by Mo/Al. Spectral analysis, however, does not show as strong a relationship between V/Al and $\delta^{18}O$ and percent TOC at the higher frequencies. Unlike the case with Mo, previous studies have also shown a lack of consistent decreases in dissolved V across the O_2-H_2S boundaries of anoxic basins [e.g., *Emerson and Huested*, 1991]. In sediments, this limitation of the V records most likely reflects the refractory terrigenous contribution of V (that is, V_{PAAS} = 150 ppm) [*Taylor and McLennan*, 1985]. As a large fraction of the total V inventory, the refractory terrigenous V serves to obscure the redox-sensitive V component.

There are strong relationships among Mo/Al, V/Al, and percent TOC in these Cariaco sediments. At all Milankovitch frequencies, when there is a statistically significant coherence, Mo/Al and V/Al are exactly in phase with percent TOC (within uncertainty, Table 1). This correlation is identical to what is observed in the shorter high-resolution record (Figure 3), which speaks to the consistent behavior of the geochemical system at the different timescales. Assuming that the elevated percent TOC results from high productivity [*Peterson et al.*, 1991, 1999; *Haug et al.*, 1998; *Werne et al.*, 2000], these strong ties support the conclusion that high productivity and the associated oxygen demand are the cause of the increase in anoxia.

Mn/Al is coherent and in phase with $\delta^{18}O$ at the 100 kyr frequency. Mn/Al maxima occur during glacial periods, which likely reflects the retention of primary detrital Mn and, therefore, oxic bottom water conditions [*Scoullos*, 1983; *Jacobs et al.*, 1987; *Landing and Bruland*, 1987; *Burton and Statham*, 1988; *Calvert and Pedersen*, 1993; *Piper*, 1994; *Crusius et al.*, 1996]. Although we cannot differentiate on the basis of bulk chemistry whether these relatively Mn-rich phases are Mn oxides, Mn sulfides, or Mn carbonates, the presence of the higher Mn nonetheless indicates a relatively oxygen-rich depositional system. In the 100 kyr band, Mn/Al data indicate that maximum oxic conditions coincide with times of minimum sea level (maximum $\delta^{18}O$). Spectral analysis shows a significant lead of Mn/Al over positive $\delta^{18}O$ in the 41 kyr band, suggesting that oxic conditions in the water column precede maximum ice volume at this frequency. As sea level lowered, resulting in increased basin isolation and a decreased influx of nutrient-rich water, both production and the removal of dissolved oxygen from the water column correspondingly decreased.

Fe/Al tends to be noncoherent or only weakly coherent with $\delta^{18}O$ and percent TOC at many frequencies. As we inferred for V (see above), the inconsistent behavior of Fe/Al most likely reflects the higher relative concentration of refractory Fe in terrigenous matter (Fe_{PAAS} ~45,000 ppm) [*Taylor and McLennan*, 1985] and the retention of reactive Fe as iron sulfide under anoxic conditions. Despite the fact that Fe variations therefore most likely reflect both a redox and provenance signal, the bulk Fe/Al generally confirms Mn/Al interpretations, indicating that the redox component of the Fe record is not totally obscured by the detrital inventory. Fe/Al and Mn/Al are in phase only at the 100 kyr frequency, which further suggests the dominance of 100 kyr forcing.

The cross-spectral analyses indicate that the oxygenation state of the Cariaco Basin is varying in concert with climate state. The relationships shown in Figure 7 and Table 1 suggest that the percent TOC, Mo/Al, and V/Al records are responding to the lack of oxygen in the bottom waters at both the 100 kyr and 41 kyr Milankovitch frequencies. In the 23 kyr and 19 kyr

bands, however, there are fewer statistically significant coherencies (Table 1), and the phase relationships (Figure 7) are not as clearly observed as they are in the 100 kyr and 41 kyr bandwidths. At the two higher frequencies, in particular, the Mo/Al (or V/Al) and Fe/Al signals, which in the 100 kyr and 41 kyr bands were oscillating in opposition, are instead much closer to each other in phase angle (Figure 7). This indicates that at these higher frequencies other processes are operating to regulate the distributions of redox-sensitive trace metals. Elucidation of which exact process is dominant within these frequencies is beyond the scope of this paper, but possibilities include provenance changes (particularly for the Fe and V records, which are the most sensitive to such changes) or local diagenetic redistribution of the trace elements (e.g., Figure 3), which will be most important over short stratigraphic distances that are statistically sampled by the higher-frequency cross-spectral analysis.

Results from this and previous research indicate a predominant sea level control on sedimentary redox chemistry, primary production, and $\delta^{15}N$ in the Cariaco Basin over the past 578,000 years. The fact that the redox metal distributions show their greatest spectral strength at 100 kyr and 41 kyr speaks to the significance of sea level change on influencing the climate record of the Cariaco Basin. *Yarincik et al.* [2000] showed, on the basis of detrital ratios Al/Ti and K/Al, that eolian source variations as well as sea level change also controls terrigenous deposition in the Cariaco Basin. During glacial times, increased influx of eolian rutile sourced from the Sahara Desert, along with an increase in the local supply of kaolinite, dominate the terrigenous sedimentary component [*Yarincik et al.*, 2000]. The unique hydrography of the Cariaco Basin, governed by the surrounding shallow sills and ultimately regulated by climate, has a profound impact on the chemistry of both the water column and the sedimentary record.

7. Conclusions

Variations in the bottom water oxygen content of the Cariaco Basin are related to glacial-interglacial cycles. High production during interglacials, as indicated by high percent TOC [*Peterson et al.*, 1991, 1999; *Haug et al.*, 1998; *Werne et al.*, 2000], results in the removal of dissolved oxygen from the water column more rapidly than it can be replenished. The resulting anoxia enriches the sediment in Mo and V (documented by elevated sedimentary Mo/Al and V/Al), given the decreased solubility of both elements under reducing conditions. During glacial periods, primary production decreased, and oxic conditions were restored in the water column, as indicated by low percent TOC [*Haug et al.*, 1998; *Peterson et al.*, 1999]. This transition leads to better preserved primary signals and the relative enrichments of Mn and Fe (higher sedimentary Mn/Al and Fe/Al values), which have decreased solubility under oxic conditions.

We have shown here that the combination of relatively simple bulk chemical analyses and robust time series analyses can illuminate local (and perhaps global) effects of climate change on sedimentation in the Cariaco Basin. The redox chemistry examined in the present study supports and strengthens previous conclusions regarding the paleohydrography and paleoceanography of the Cariaco Basin and in particular emphasizes the role of sea level change in regulating the climate record within the basin. Though much of this study addresses the relatively low Milankovitch frequencies of climate change, it provides a template for chemical studies at higher, sub-Milankovitch timescales.

Acknowledgments. We thank Dave Murray at Brown University for great help during this research project. His insight is greatly appreciated. Several anonymous reviewers also made suggestions that improved upon our efforts. R.W.M., T.W.L., and L.C.P. acknowledge financial support from USSSP postcruise funding and from NSF grant OCE-9709807 (to L.C.P.). G.H.H. was funded by the German Science Foundation (DFG) and NSERC (Canada). Samples were provided by the Ocean Drilling Program. Acquisition and initial maintenance of the JY170C ICP-ES facility at Boston University was supported by NSF EAR-9724282. K.M.Y. thanks Boston University for graduate student support. We thank Adila Jamil, Martha Evonuk, and Joel Sparks for their assistance in the Analytical Geochemistry Laboratory at Boston University.

References

Breit, G. N., and R. B. Wanty, Vanadium accumulation in carbonaceous rocks: A review of geochemical controls during deposition and diagenesis, *Chem. Geol., 91*, 83-97, 1991.

Burton, J. D., and P. J. Statham, Trace metals as tracers in the ocean, in *Tracers in the Ocean*, edited by H. Charnock et al., pp. 127-145, Princeton Univ. Press, Princeton, N. J., 1988.

Calvert, S. E., and T. F. Pedersen, Geochemistry of Recent oxic and anoxic marine sediments: Implications for the geologic record, *Mar. Geol., 113*, 67-88, 1993.

Canfield, D. E., Reactive iron in marine sediments, *Geochim. Cosmochim. Acta, 53*, 619-632, 1989.

Canfield, D. E., R. Raiswell, and S. Bottrell, The reactivity of sedimentary iron minerals toward sulfide, *Am. J. Sci., 292*, 659-683, 1992.

Canfield, D. E., T. W. Lyons, and R. Raiswell, A model for iron deposition to euxinic Black Sea sediments, *Am. J. Sci., 296*, 818-834, 1996.

Crusius, J., S. Calvert, T. Pedersen, and D. Sage, Rhenium and molybdenum enrichments in sediments as indicators of oxic, suboxic and sulfidic conditions of deposition, *Earth Planet. Sci. Lett., 145*, 65-78, 1996.

Dean, W. E., J. V. Gardner, D. Z. Piper, Inorganic geochemical indicators of glacial-interglacial changes in productivity and anoxia on the California continental margin, *Geochim. Cosmochim. Acta*, 61, 4507-4518, 1997.

Dean, W. E., D. Z. Piper, and L. C. Peterson, Molybdenum accumulation in Cariaco Basin sediment over the past 24 kyr: A record of water-column anoxia and climate, *Geology, 27*, 507-510, 1999.

Deuser, W. G., Oxidation of organic matter and residence time of anoxic water, *Nature, 242*, 601-603, 1973.

Dymond, J., R. Collier, J. McManus, S. Honjo, and S. Manganini, Can the aluminum and titanium contents of ocean sediments be used to determine the paleoproductivity of the oceans?, *Paleoceanography, 12*, 586-593, 1997.

Emerson, S. R., and S. S. Huested, Ocean anoxia and the concentrations of molybdenum and vanadium in seawater, *Mar. Chem., 34*, 177-196, 1991.

Francois, R., A study on the regulation of the concentrations of some trace metals (Rb, Sr, Zn, Pb, Cu, V, Cr, Ni, Mn and Mo) in Saanich Inlet sediments, British Columbia, Canada, *Mar. Geol., 83*, 285-308, 1988.

Gruber, N., and J. L. Sarmiento, Global patterns of marine nitrogen fixation and denitrification, *Global Biogeochem. Cycles, 11*, 235-266, 1997.

Haug, G., T. F. Pedersen, D. M. Sigman, S. E. Calvert, B. Nielsen, and L. C. Peterson, Glacial/interglacial variations in production and nitrogen fixation in the Cariaco Basin during the last 580 kyr, *Paleoceanography, 13*, 427-432, 1998.

Helz, G. R., C. V. Miller, J. M. Charnock, J. F. W. Mosselmans, R. A. D. Pattrick, C. D. Garner, and D. J. Vaughan, Mechanism of molybdenum removal from the sea and its concentration in black shales: EXAFS evidence, *Geochim. Cosmochim. Acta, 60*, 3631-3642, 1996.

Hughen, K. A., J. T. Overpeck, L. C. Peterson, and R. G. Anderson, The nature of varved

sedimentation in the Cariaco Basin, Venezuela, and it's palaeoclimatic significance, in *Palaeoclimatology and Palaeoceanography from Laminated Sediments*, edited by A. E. S. Kemp, *Geol. Soc. Spec. Publ., 116*, 171-183, 1996a.

Hughen, K., J. T. Overpeck, L. C. Peterson, and S. E. Trumbore, Rapid climate changes in the tropical Atlantic during the last deglaciation, *Nature, 380*, 51-54, 1996b.

Imbrie, J., J.D. Hays, D.G. Martinson, A. McIntyre, A.C. Mix, J.J. Morley, N.G. Pisias, W.L. Prell, and N.J. Shackleton, The orbital theory of Pleistocene climate: Support from a revised chronology of the marine $\delta^{18}O$ record, in *Milankovitch and Climate, Part 1*, edited by A.L. Berger et al., pp. 269-305, D. Reidel, Norwell, Mass., 1984.

Imbrie, J., et al., On the structure and origin of major glaciation cycles, 1. Linear responses to Milankovitch forcing, *Paleoceanography, 7*, 701-738, 1992.

Jacobs, L., S. Emerson, and S. S. Huested, Trace metal geochemistry in the Cariaco Trench, *Deep Sea Res., 34*, 965-981, 1987.

Jones, B., and D. A. C. Manning, Comparison of geochemical indices used for the interpretation of palaeoredox conditions in ancient mudstones, *Chem. Geol., 111*, 111-129, 1994.

Landing, W. M., and K. W. Bruland, The contrasting biogeochemistry of iron and manganese in the Pacific Ocean, *Geochim. Cosmochim. Acta, 51*, 29-43, 1987.

Lin, H.-L., L. C. Peterson, J. T. Overpeck, S. E. Trumbore, and D. W. Murray. Late Quaternary climate change from $\delta^{18}O$ records of multiple species of planktonic foraminifera: High-resolution records from the anoxic Cariaco Basin, Venezuela, *Paleoceanography, 12*, 415-427, 1997.

Lyons, T. W., Sulfur isotopic trends and pathways of iron sulfide formation in upper Holocene sediments of the anoxic Black Sea, *Geochim. Cosmochim. Acta, 61*, 3367-3382, 1997.

Lyons, T. W., and R. A. Berner, Carbon-sulfur-iron systematics of the uppermost deep-water sediments of the Black Sea, *Chem. Geol.,99*, 1-27, 1992.

Lyons, T. W., J. P. Werne, D. J. Hollander, R. W. Murray, D. G. Pearson, L. C. Peterson, and ODP Leg 165 Shipboard Scientific Party, Biogeochemical pathways in Holocene and latest Pleistocene sediments of the anoxic Cariaco Basin: Linkages to palaeoceanographic and palaeoclimatic variability, *Mineral. Mag., 62A*, 931-932, 1998.

Morford, J. L., and S. Emerson, The geochemistry of redox sensitive trace metals in sediments, *Geochim. Cosmochim. Acta, 63*, 1735-1750, 1999.

Murray, R. W., and M. Leinen, Scavenged excess aluminum and its relationship to bulk titanium in biogenic sediment from the central equatorial Pacific Ocean, *Geochim. Cosmochim. Acta, 60*, 3869-3878, 1996.

Peterson, L. C., J. T. Overpeck, N. G. Kipp, and J. Imbrie, A high-resolution late Quaternary upwelling record from the anoxic Cariaco Basin, Venezuela, *Paleoceanography, 6*, 99-119, 1991.

Peterson L. C., G. H. Haug, R. W. Murray, K. M. Yarincik, J. W. King, T. J. Bralower, K. Kameo, and R. B. Pearce, Late Quaternary stratigraphy and sedimentation at ODP Site 1002, Cariaco Basin (Venezuela), *Proc. Ocean Drill. Program Sci. Res., 165*, 85-99, 1999.

Piper, D. Z., Seawater as the source of minor elements in black shales, phosphorites and other sedimentary rocks, *Chem. Geol., 114*, 95-114, 1994.

Piper, D. Z., and C. M. Isaacs, Minor elements in Quaternary sediment from the Sea of Japan: A record of surface-water productivity and intermediate-water redox conditions, *Geol. Soc. Am. Bull., 107*, 54-67, 1995.

Raiswell, R., and D. E. Canfield, Sources of iron for pyrite formation in marine sediments, *Am. J. Sci., 298*, 219-245, 1998.

Schubert, C., The origin of the Cariaco Basin, southern Caribbean Sea, *Mar. Geol., 47*, 345-360, 1982.

Scoullos, M. J., Trace metals in a landlocked intermittently anoxic basin, in *Trace Metals in Sea Water*, edited by C. S. Wong et al., pp. 351-366, Plenum, New York, 1983.

Sigurdsson, H., et al., *Proceedings of the Ocean Drilling Program, Initial Reports*, vol. 165, Ocean Drill. Program, College Station, Tex., 1997.

Taylor, S. R., and S. M. McLennan, *The Continental Crust: Its Composition and Evolution*, Blackwell Sci., Malden, Mass., 1985.

Walsh, J. J., Nitrogen fixation within a tropical upwelling ecosystem: Evidence for a Redfield budget of carbon/nitrogen cycling by the total phytoplankton community, *J. Geophys. Res., 101*, 607-620, 1996.

Werne, J. P., D. J. Hollander, T. W. Lyons, and L. C. Peterson, Climate-induced variations in productivity and planktonic ecosystem structure from the Younger Dryas to Holocene in the Cariaco Basin, Venezuela, *Paleoceanography, 15*, 19-29, 2000.

Yarincik, K. M., Eolian, hemipelagic, and redox-controlled deposition in the Cariaco Basin, Venezuela, over the past 578,000 years, M.A. thesis, Boston Univ., Boston, Mass., 1999.

Yarincik, K. M., R. W. Murray, and L. C. Peterson, Climatically controlled eolian and hemipelagic deposition in the Cariaco Basin, Venezuela, over the past 578,000 years: Results from Al/Ti and K/Al, *Paleoceanography, 15*, 210-228, 2000.

Zhang, J.-Z., and J. J. Millero, The chemistry of anoxic waters in the Cariaco Trench, *Deep Sea Res., Part I, 40*, 1023-1041, 1993.

G. H. Haug, Department of Earth Sciences, ETH-Zentrum, Sonneggstrasse 5, CH8092 Zurich, Switzerland. (haug@erdw.ethz.ch)

T. W. Lyons, Department of Geological Sciences, University of Missouri, Columbia, MO 65211. (lyonst@missouri.edu)

R. W. Murray and K. M. Yarincik, Department of Earth Sciences, Boston University, Boston, MA 02215. (rickm@bu.edu; yarincik@bu.edu)

L. C. Peterson, Rosenstiel School of Marine and Atmospheric Science, University of Miami, Miami, FL 33149. (lpeterson@rsmas.miami.edu)

(Received May 1, 1999;
revised June 15, 2000;
accepted June 20, 2000.)